FEBRUARY 2017

APPLICATIONS OF PORTABLE RAMAN SPECTROSCOPY

Sponsored by
B&W TEK
Your Spectroscopy Partner

Presented in partnership with
Spectroscopy
UBM

TOC
Table of contents

APPLICATIONS OF PORTABLE RAMAN SPECTROSCOPY

Spectroscopy

UBM

THE VERSATILITY OF PORTABLE RAMAN IN PROCESS DEVELOPMENT

Thomas Padlo and Katherine Bakeev

Raman spectroscopy is a well-suited spectroscopic technique for process development and control within development laboratories in chemical, pharmaceutical, and other industries. This article demonstrates the utility of portable Raman spectroscopy as a simple and versatile tool for in-situ monitoring of reactions using univariate analysis techniques such as peak trending, as well as multivariate analysis approaches to predict the end point of chemical reactions. The use of portable Raman systems allows analysts to make measurements in the laboratory, but also serves as a proof of concept for the Raman measurements to be implemented at-line or on-line in small pilot plants or large-scale production sites. For known reactions that are repetitively performed, or for continuous on-line process monitoring of reactions, the present approach provides a convenient solution for process understanding as well as a basis for future implementation.

Process analytics has been in use for nearly 70 years, starting in the petrochemical and chemical industries using infrared (IR) photometers and different types of devices such as oxygen and conductivity sensors as process analyzers to control manufacturing and refining processes (1). These univariate sensors and others continue to be used, and other sensors including spectroscopic systems have also been adopted. The value of process analytics is that it can provide the pulse of a process. *Process analytical technology (PAT)* is the use of off-line, at-line, or in-line analyzers to obtain analytical data faster, more often with high precision to increase manufacturing controls of biological or chemical materials, as well as aid in process understanding for optimization and improvement (2). PAT has seen increased interest since 2005 with the publication of a guidance on PAT utilization in the pharmaceutical industry from the United States Food and Drug Administration (FDA). Spectroscopic tools including Raman can be used in situ or can be interfaced to a sampling loop on a process to monitor the chemical composition with full spectral information, which is the molecular picture of the changes occurring in the process. The amount of data that can be collected may exceed the speed of a process and in the early phases of process development this can be used to understand a process and its dynamics, possible side reactions, and kinetic pathways.

Raman spectroscopy is a laser-based form of molecular spectroscopy that provides specificity and sensitivity for qualitative and quantitative analysis of substances from their molecular

vibrations. It is used in many different environments as an analytical tool for the study of solids, liquids, and gases. Many Raman instruments are interfaced with a fiber-coupled probe, which gives the versatility and flexibility for measurements to be made in different places, including in situ as is often the requirement for the monitoring of processes. More than a decade ago, hardware developments that lead to an increase in the adoption of Raman spectroscopy were recognized as the development of compact lasers, introduction of spectroscopic-grade charge-coupled device detectors, improvements in sampling optics (including fiber-optic probes), and the advances in powerful personal computers and associated software to collect and analyze volumes of data (3). These developments, as well as the advancement of technology in laser and spectrometer miniaturization and improved filters for laser light rejection and fiber-optic probes, have allowed for the development of portable Raman spectroscopy systems that can be deployed and transported to different locations for uses that include process analysis. There are other complementary spectroscopic techniques to Raman such as Fourier transform infrared (FT-IR) and near-infrared (NIR) spectroscopy. However, because of Raman spectroscopy's flexible sampling interface, high sampling rate, and high spectral specificity it is an invaluable tool for qualitative and quantitative analysis of chemical systems for reaction monitoring and end-point detection for chemical synthesis and polymerization reactions, hydrogenation, hydrolysis, and polymorphic characterization (1,3,5).

In the development of a process,

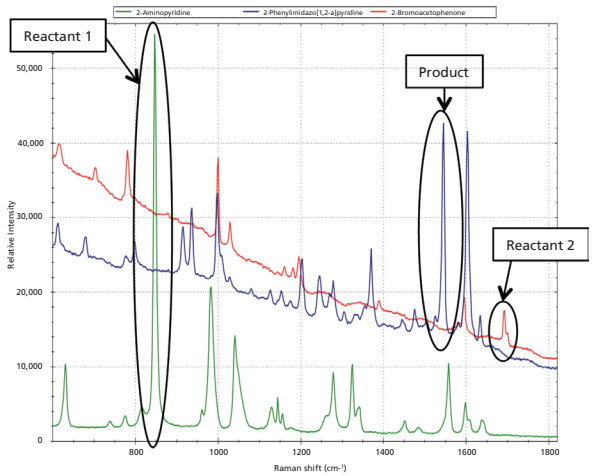

Figure 1: Overlay of the Raman spectra of the reactants and product for the first synthesis: green = 2-aminopyridine (reactant), red = 2-bromoacetophenone (reactant), and blue = final product: 2-phenylimidazo[1,2-a]pyridine.

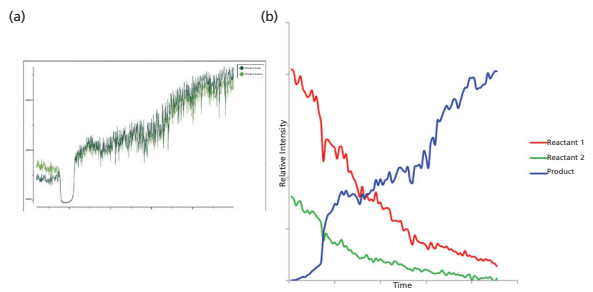

Figure 2: (a) Real-time peak trending of the two product peaks during the course of the reaction and (b) univariate peak trending plots using the (second derivative *-1 to remove any variation that might be coming from the baseline): red = 2-bromoacetophenone (reactant 1), green = 2-aminopyridine (reactant 2), and blue = final product: 2-phenylimidazo[1,2-a]pyridine synthesis.

there are many parameters that may be evaluated and experiments performed to optimize the yield, purity, and cycle time. To understand the impact of process changes on the process and product, in situ measurements can be made that relate the process parameters to product and process properties.

In choosing measurement tools in process development, the needs of the chemical system in terms of "purpose, specificity, sensitivity, cycle time, on-line–off-line, qualitative–quantitative, accuracy, precision" must be defined and the proper technology that can fulfill the defined criteria must be chosen (4). In early phases of process development, qualitative information on reaction progress may be sufficient to gauge reaction completion. The trending of reactant- and product-relative concentrations based on peak height or area in a spectrum can be used to follow a reaction, even as other reaction parameter (such as solvent and other reagents or temperature) are changed from one reaction to another. In reactions where stoichiometric control is required, a quantitative measure of reactant concentrations may be needed. Off-line measurements by high performance liquid chromatography (HPLC) can be made and quantitative calibration models developed, but such models are matrix dependent and often require updating or redevelopment when the reaction matrix is changed.

In this study, the goal was to determine the end point of the chemical reaction for the 6-methyl-2-phenylimidazo[1,2-a] pyridine synthesis and its derivative. The synthesis of this compound was under development for medicinal chemistry, and traditional thin-layer chromatography (TLC) was used to verify reaction completion, but very few aliquots are taken at the small-scale reactions, and the timing for sampling for the end point is based on the visual precipitation in the reaction mixture followed by the TLC test. Information on reaction progress

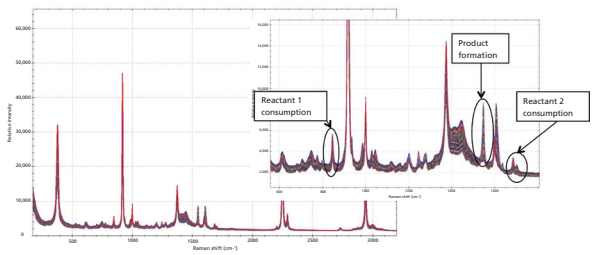

Figure 3: Reaction monitoring data for the first univariate test run. Note the consumption of the two reactant peaks at 847 cm^{-1} (reactant 1) and the broad band between 1684–1702 cm^{-1} (reactant 2) as well as the formation of the product at 1547 cm^{-1}.

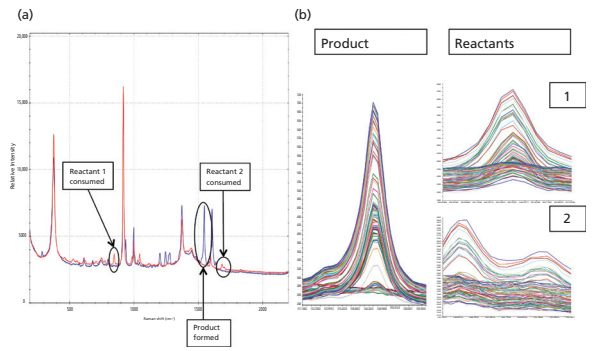

Figure 4: (a) The first and last spectra of the reaction along with (b) the peak trends of the formation of the product and the consumption of the reactants.

and possible formation of intermediates and side products is possible only when Raman spectra are collected regularly throughout the course of the reaction. Monitoring the reaction with in situ Raman spectroscopy reduces the need for removing samples for analysis and also provides real-time information on reaction progress.

Experimental

The experimental setup consisted of an i-Raman Plus portable Raman spectrometer from B&W Tek with a 785-nm, 300-mW laser excitation source connected to a back-thinned charge-coupled device (CCD) array detector covering a spectral range of 65–3200 cm^{-1}. The sampling interface was a fiber-optical bundle with an immersion probe to allow for in situ measurements during the reactions. The Raman instrument was used to monitor the small molecular synthesis of 6-methyl-2-phenylimidazo[1,2-a]pyridine synthesis and its derivative 2-phenylimidazo[1,2-a]pyridine. The immersion probe was inserted into the round-bottom flask for direct measurement throughout the course of the reaction. The starting reagents were suspended into acetonitrile, and a small amount of sodium bicarbonate was added to neutralize the hydrobromic acid that formed during the process. The reaction was placed under argon atmosphere and heated to 80 °C for approximately 2 h. Raman measurements were collected every minute during the reaction with an integration time of 3 s averaged over 10 spectra.

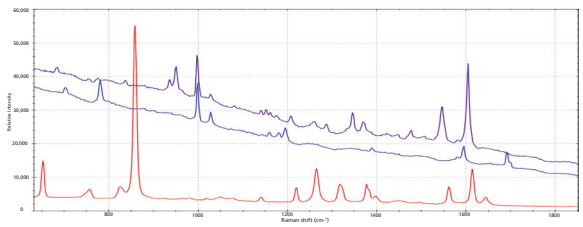

Figure 5: Overlay of reactants and product for the MCR approach: red = 2-amino-5-methyl-pyridine (reactant), blue = 2-bromoacetophenone (reactant), and purple = final product 6-methyl-2-phenylimidazo[1,2-a]pyridine.

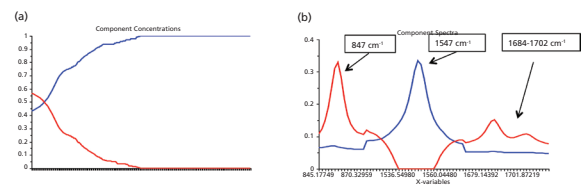

Figure 6: (a) The two component spectra and (b) two component concentration of the MCR results.

Two similar S_n2 reactions were monitored to understand the reactions and determine their reaction end point. In these chemical reactions for development of these medicinal chemistry compounds, the goal of the process monitoring was to have a qualitative trend of the reaction progress and a means to detect the reaction end point. The first reaction is 2-aminopryidine reacted with 2-bromoacetophenone to form 2-phenylimidazo[1,2-a]pyridine. For this reaction, a univariate approach of monitoring the reactant and product peaks was conducted using B&W Tek's BWSP software. For the second reaction of 2-amino-5-methyl-pyridine and 2-bromoacetophenone to form 6-methyl-2-phenylimidazo[1,2-a]pyridine, a

multivariate analysis method was applied using the Unscrambler software (CAMO Software). This approach also provided qualitative information, because there was no requirement of quantitation, but rather a real-time measure of reaction end point in place of previously used off-line TLC.

Results and Discussion

For the first reaction of the synthesis of 2-phenylimidazo[1,2-a]pyridine, a spectrum was taken for each of the starting materials and the final product to identify the Raman peaks to monitor during the course of the reaction process. As shown in Figure 1, the three regions of interest are 847 cm^{-1} (2-aminopyridine, reactant 1), 1547 cm^{-1} (final product), and broad dual peaks between 1684 and 1702 cm^{-1} (2-bromoacetophenone, reactant 2). Because of the specificity of the Raman spectrum and the fact that these identified peaks do not have any overlap with other Raman peaks of solvent or other reaction components, univariate analysis can be effectively used. During the progression of the reaction the two product peaks at 1547 cm^{-1} and 1603 cm^{-1}, respectively, were monitored as shown in Figure 2a. The region with a significant dip in the real-time trending plot of relative intensity as a function of time was caused by probe fouling. This fouling can occur during in situ monitoring because material may adhere to the probe, and for full process monitoring implementations a measure should be taken to minimize it, including better control of stirring or automated probe cleaning procedures. Figure 2b is the peak trending plot of the reactants and product peaks created post-reaction with the probe fouling data removed. The data plotted was preprocessed using a second order derivative Savitzky-Golay filter to minimize baseline effects; the data were then multiplied by -1 to reverse the trend in the plot to show the reactants decreasing and product peaks increasing. The Raman spectra collected throughout the reaction monitoring are shown in Figure 3, with the reactant peaks visibly diminishing while the product peak is simultaneously increasing as the reaction progresses. The univariate analysis provided supportive information into the end point of the reaction as shown in Figure 4a where the overlay of the first and last spectra from the reaction illustrate the complete consumption of the reactants. Based on the peak trending plots of the reactants and product (Figure 2b), along with the overlay the first and last spectra collected (Figure 4a), the reaction appears to finish within 2 h. On a closer observation of the overlay regions of interest, shown in Figure 4b, the data indicates the reaction could have come to completion sooner because the peaks for the reactants are not visible in the raw data before the last collected spectrum.

For the second reaction of the synthesis of 6-methyl-2-phenylimidazo[1,2-a] pyridine, the spectra of each starting material and final product were collected and the peaks of interest were identified for the reaction monitoring. The peaks were the same as the previous reaction, 847 cm^{-1} (2-amino-5-methyl-pyridine,

reactant 1), 1547 cm^{-1} (final product), and broad dual peaks between 1684–1702 cm^{-1} (2-bromoacetophenone, reactant 2), as shown in Figure 5. The reaction proceeded for around 2 h with data collected throughout the course of the reaction at 1 min intervals. The peak trending during the course of the reaction showed similar profiles as those generated for the first reaction and gave insight into reaction progress. After the reaction, further data analysis was performed on the collected data using exploratory multivariate analysis. A multivariate curve resolution alternating least squares (MCR-ALS) algorithm was applied using the Unscrambler software over the regions of interest that include the product and reactant peaks. By this analysis, a two-component concentration and two-component spectra were determined, shown in Figure 6. The two component spectra were indicative to the product and reactant spectra. They are consistent with the reference spectra collected of the starting materials and product. The computed profiles plateau about midway through the reaction data collection, indicating that it was actually over in half the time, around 1 h. The experiments were repeated and validated using TLC to confirm the reaction completion in 1 h. The Raman spectroscopic monitoring of the reaction provided information on the reaction progress, and resulted in reducing the reaction cycle time by half.

Conclusions

Raman spectroscopy for process analytics is an invaluable tool for understanding reactions that have significant benefits for the chemical, pharmaceutical, and other industries. The aim of this contribution was to demonstrate the ability for portable Raman spectroscopy coupled with univariate and multivariate analysis tools in the process development stage to gain insight and process understanding of chemical reactions, specifically in determining reaction end points, on a laboratory-scale setup. The Raman spectral data was valuable to monitor the reaction qualitatively. These experiments serve as a proof of concept for further development with Raman measurements to move forward with at-line or on-line implementation as the chemical process is scaled up to pilot and manufacturing scales. This work demonstrates the versatility and ability of portable Raman spectrometers and their utility in process development and understanding.

References

(1) *Process Analytical Technology: Spectroscopic Tools and Implementation Strategies for the Chemical and Pharmaceutical Industries,* 2nd Edition, K.A. Bakeev, Ed. (John Wiley & Sons, Ltd., West Sussex UK, 2010).
(2) US Food and Drug Administration, *Guidance for Industry: PAT — A Framework for Innovative Pharmaceutical Development, Manufacturing, and Quality Assurance* (FDA, Rockville, Maryland, 2004).
(3) J.B. Slater, J.M. Tedesco, R. Fairchild, and I.R. Lewis, in *Handbook of Raman Spectroscopy,* I.R. Lewis and H.G.M. Edwards, Eds. (CRC Press, New York, New York, 2001).
(4) G.L. Reid et al., *Am. Pharm. Rev.* June 20 (2012).
(5) X. Chen et al., *Org. Process Res. Dev.* **19**(8), 995–1003 (2015).

Thomas Padlo and **Katherine Bakeev** are with B&W Tek in Newark, Delaware. Direct correspondence to: thomasp@bwtek.com and katherineb@bwtek.com

This article originally appeared in *Spectroscopy, **31**(s9),* 16–22 (2016).

LIBRARY-BASED SCREENING OF PHARMACEUTICAL MATERIALS BY HANDHELD RAMAN AND NEAR-INFRARED SPECTROMETERS

Chelliah V. Navin, Latevi S. Lawson, and Jason D. Rodriguez

The availability of quality drugs is crucial in the event of a pandemic. Here, we report our pilot efforts to perform rapid screening of anti-infective drugs for confirmation of drug product quality using near-infrared (NIR) and Raman library methods. The methods reported are nondestructive toward the sample and are designed to facilitate rapid physical testing of drugs at the point of use or in a field setting. We built a representative library through voluntary collaboration with six manufacturers of antibiotic and antiviral drugs. The drugs supplied by these manufacturers are representative of imported United States Food and Drug Administration (FDA) approved finished products. We successfully transferred the spectral libraries from laboratory-based instruments to field-deployable handheld NIR and Raman instruments and challenged the library methods using independent samples from different batches.

Anti-infective medicines such as antibacterial and antiviral drugs play an important role during a pandemic outbreak (1). In an effort to promote nondestructive screening of anti-infective drugs, the United States Food and Drug Administration (FDA) Division of Pharmaceutical Analysis (DPA) has developed spectral library–based approaches (2,3) for confirmation of drug product quality on portable spectrometers. Spectral libraries can be used to screen counterfeit products by comparing them against spectral signatures of authentic finished drug products (4–6). In this article, we report our attempt to screen common anti-infective drugs, such as those that would be used during an emergency situation like a global pandemic, using spectral libraries built and transferred from laboratory-based instruments to handheld near-infrared (NIR) and Raman spectrometers. The methods developed are easy to use by nonexperts and provide the opportunity to screen materials based on pass–fail determinations (7). Typically, these techniques are fast and deliver results in less than 60 s, thereby streamlining the process of performing analysis on finished drug products (6). In addition, these nondestructive approaches require no sample preparation and can analyze a sample directly through a transparent container or blister packaging (8–13).

Methods

A list of antibacterial and antiviral drugs used to build the master library is provided in Table I. A total of 150 finished drug product samples (including different batches and dosage strengths) from six generic drug manufacturers were included in the study. The samples were received on a voluntary basis directly from the manufacturers. The laboratory NIR spectrometer used to build the library was an Antaris II Fourier transform NIR spectrometer (Thermo Fisher Scientific). Spectral collection for the library entries was performed using the integrating sphere assembly at 4000–10,000 cm^{-1} at 8 cm^{-1} resolution and a gain of 1×. Each spectrum collected consisted of 32 scans. The laboratory Raman spectrometer used to build the library was a Kaiser Raman Workstation 785 nm (Kaiser Optical Systems Inc.). The Raman 3-mm wide-beam probe assembly was used to collect the spectra and the total collection time for each spectrum was 30 s (1 s integration × 30 scans). The laser power at the sample was ~250 mW.

The spectrum used in the NIR and Raman master libraries was the average of multiple tablets or capsules taken from each sample received. The average spectrum for each sample was obtained by randomly sampling six tablets or capsules from each sample bottle. Each tablet or capsule was analyzed twice, one spectrum for each side in the case of tablets and two random orientations for capsules. The same exact tablets and capsules were analyzed by both NIR and Raman libraries. The resulting 12 spectra for each tablet and capsule were averaged into a single entry for each spectral library.

The NIR and Raman libraries were transferred to handheld instruments

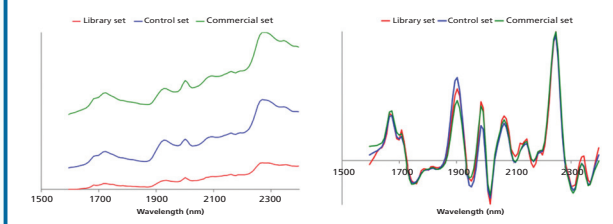

Figure 1: Left: Comparison of NIR spectra for famciclovir. The spectra have been offset for clarity. Right: Comparison of first derivative spectra for famciclovir. All spectra have been normalized to facilitate visual comparison.

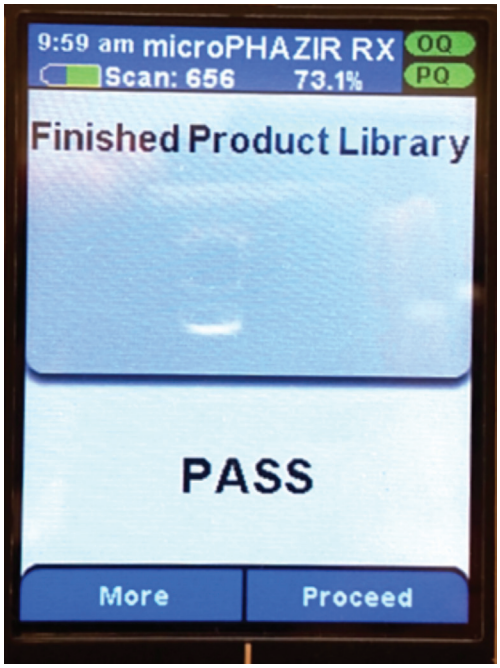

Figure 2: Typical handheld NIR spectrometer result screen indicating a "Pass" for the famciclovir test set.

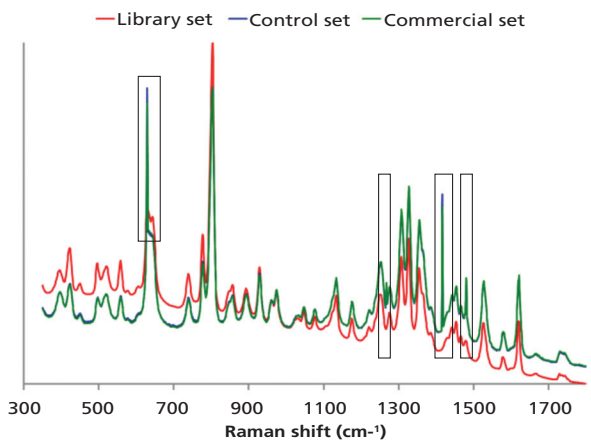

Figure 3: Raman spectral plot comparison of famciclovir with hot pixels indicated by the black boxes.

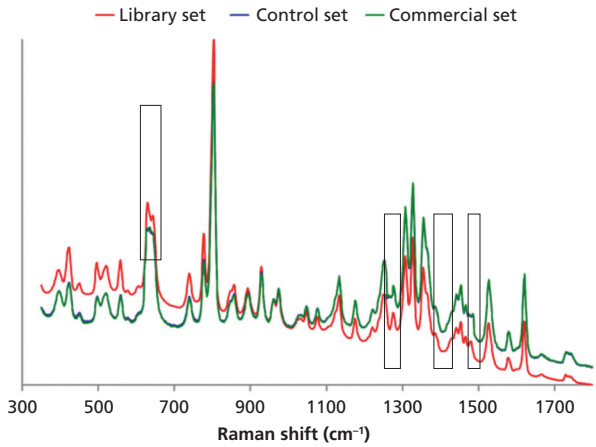

Figure 4: Raman spectral plot comparison of famciclovir without hot pixels. The black box indicates the locations where the hot pixels were seen before elimination.

Table I: Antibacterial and antiviral drugs obtained from Indian pharmaceutical companies

Finished Pharmaceutical Drug		Source
Acyclovir	400 mg	Manufacturer 5
Ciprofloxacin	250 mg	Manufacturer 1
Ciprofloxacin	500 mg	Manufacturer 1
Ciprofloxacin	500 mg	Manufacturer 2
Cephalexin	250 mg	Manufacturer 4
Clarithromycin	250 mg	Manufacturer 1
Clarithromycin	500 mg	Manufacturer 1
Famciclovir	250 mg	Manufacturer 3
Famciclovir	500 mg	Manufacturer 3
Famciclovir	125 mg	Manufacturer 6
Famciclovir	250 mg	Manufacturer 6
Famciclovir	500 mg	Manufacturer 6
Famciclovir	125 mg	Manufacturer 5
Levofloxacin	250mg	Manufacturer 2
Levofloxacin	750 mg	Manufacturer 2
Levofloxacin	250 mg	Manufacturer 4
Levofloxacin	500 mg	Manufacturer 4
Levofloxacin	750 mg	Manufacturer 4
Metronidazole	500 mg	Manufacturer 3
Minocycline	100 mg	Manufacturer 1
Minocycline	75 mg	Manufacturer 1
Minocycline	50 mg	Manufacturer 1
Minocycline HCl	50 mg	Manufacturer 3
Minocycline HCl	75 mg	Manufacturer 3
Minocycline HCl Extended Release	90 mg	Manufacturer 5
Minocycline HCl Extended Release	135 mg	Manufacturer 5
Valacyclovir	1000 mg	Manufacturer 1
Valacyclovir	1000 mg	Manufacturer 1
Valacyclovir	500 mg	Manufacturer 2
Valacyclovir	1000 mg	Manufacturer 2
Valacyclovir HCl	500 mg	Manufacturer 6
Valacyclovir HCl	1000 mg	Manufacturer 6
Valacyclovir HCl	500 mg	Manufacturer 5

and the performance of the library was challenged by assembling three different test sets. The test sets consisted of

- the batch used for library development (master);
- a different batch received through the manufacturer submitting the library lot (control); and
- the same product procured in the United States through a commercial distributor (commercial).

Each test set included 10 drug products, which are listed in Table II. Spectral measurements were acquired on each of the 10 sample test sets using a handheld Phazir NIR spectrometer (Thermo Scientific) in the 1595-2400 nm

Table II: Spectral correlation values calculated for the control and commercial sets using a handheld NIR spectrometer

Pharmaceutical Drug	Manufacturer Number	SC Values for NIR		NIR Determination	
		Control Set	Commercial Set	Control Set	Commercial Set
Ciprofloxacin	1	0.988	0.988	Pass	Pass
Ciprofloxacin	2 (set 1)	0.984	0.984	Pass	Pass
Ciprofloxacin	2 (set 2)	0.984	0.984	Pass	Pass
Famciclovir	3	0.981	0.981	Pass	Pass
Levofloxacin	4 (set 1)	0.973	0.973	Pass	Pass
Levofloxacin	4 (set 2)	0.973	0.973	Pass	Pass
Levofloxacin	2 (set 1)	0.985	0.985	Pass	Pass
Levofloxacin	2 (set 2)	0.985	0.985	Pass	Pass
Metronidazole	3	0.983	0.983	Pass	Pass
Valacyclovir	5	0.989	0.989	Pass	Pass

Table III: Spectral correlation (SC) values calculated for the control and commercial sets using handheld Raman spectrometer after hot pixel elimination

Pharmaceutical Drug	Manufacturer Number	SC Values for Raman		Raman Determination	
		Control Set	Commercial Set	Control Set	Commercial Set
Ciprofloxacin	1	0.942	0.934	Pass	Pass
Ciprofloxacin	2 (set 1)	0.930	0.889	Pass	Fail
Ciprofloxacin	2 (set 2)	0.930	0.900	Pass	Pass
Famciclovir	3	0.960	0.959	Pass	Pass
Levofloxacin	4 (set 1)	0.929	0.942	Pass	Pass
Levofloxacin	4 (set 2)	0.928	0.942	Pass	Pass
Levofloxacin	2 (set 1)	0.944	0.938	Pass	Pass
Levofloxacin	2 (set 2)	0.944	0.946	Pass	Pass
Metronidazole	3	0.895	0.988	Fail	Pass
Valacyclovir	5	0.918	0.900	Pass	Pass

wavelength range. A 785–nm EZ Raman H handheld spectrometer (TSI Inc., formerly Enwave Optronics Inc.) was used to analyze the 10 sample test sets in the 350–1800 cm^{-1} range. Raman spectral collection was achieved using custom software built in-house. The software uses variable acquisition time based on a 1-s preliminary acquisition. The software is designed to optimize collection parameters to achieve a 50,000-cps intensity.

Each sample used in the test set was run multiple times (15 times for NIR and 10 times for Raman), and the average spectrum was used to compare to the library spectrum. The NIR and Raman libraries were preprocessed before distribution to the NIR and Raman instrument. The processing used for the NIR library before transfer to the handheld spectrometer was interpolation of the master library to the wavelength region used by the handheld spectrometer followed by first derivative preprocessing (second order, five-point window). The Raman library was corrected following the previously reported procedure (7) and the library and test Raman spectra were pretreated with first derivative preprocessing (second order, 31-point window) before comparison. Comparison between library and test samples was achieved by calculating the spectral correlation (SC) value according to the following equation:

$$SC = \frac{(Library \cdot Test)^2}{(Library \cdot Library)(Test \cdot Test)} \quad (1)$$

The SC value is calculated based on the correlation coefficient algorithm and the SC value ranges between 1 and 0, with 1 indicating a perfect correlation and 0 indicating a poor correlation between two different spectral measurements. In this work, a SC value of 0.90 was used as the pass–fail threshold to justify the applicability of using a spectral library generated using the handheld NIR and Raman spectrometers.

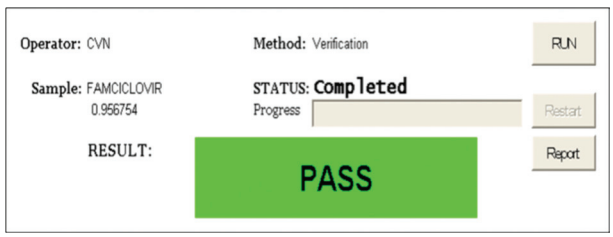

Figure 5: Handheld Raman spectrometer user interface indicating a "Pass" for one of the replicate runs in the famciclovir commercial set.

Results and Discussion

NIR spectra of the test set for a 500-mg famciclovir tablet are shown in Figure 1. The handheld NIR spectrometer was used to collect the spectral signatures of the control and commercial samples and compared against the library set spectra acquired on the benchtop NIR spectrometer. As can be seen from visual inspection of Figure 1 (left), there are slight differences between the spectra acquired by the benchtop (library set) and handheld NIR spectrometer (control and commercial sets). The differences between the spectra acquired on the benchtop and handheld units are not surprising since the benchtop instrument is a high-performance Fourier transform system and the handheld units are dispersive instruments. Some of the resolution differences can be seen in the spectra as well because the master library spectrum features slightly narrower features at ~1700 and 2000 nm. These differences are largely preprocessed when visually comparing between the smoothed first derivative spectra, which are shown in Figure 1

(right). The SC values for the famciclovir's control and commercial samples are 0.981 and 0.971, respectively, and are listed in Table II along with the NIR SC results for all the samples included in this work. An image of the handheld NIR spectrometer user interface indicating a "Pass" for the famciclovir commercial set is given in Figure 2 to demonstrate the view that would be seen by the investigator. The results for each of the 10 products in the control and commercial sets listed in Table II yield SC values greater than 0.90, which was used as the pass–fail threshold. All samples passed the screening and there was not any significant difference in the SC values between the control and commercial sets compared to the master library set. The similarity in the control and commercial SC values indicates that the spectral library signatures chosen to populate the library are representative of the supply chain for each particular drug.

Unlike the spectra acquired using the handheld NIR spectrometer, noticeable differences were observed in comparing the Raman spectra acquired on the laboratory spectrometer and handheld unit (Figure 3). Figure 3 shows a visual comparison of the spectral plots for famciclovir's control and commercial sets with the library set. Four boxes in the Raman spectra of Figure 3 show "hot pixels" present in the handheld spectrometer spectra. These hot pixels are manifested as sharp, artificial peaks in the spectra and are due to specific pixels in the detector that are close to saturation even with the laser off (14). Hot pixels add spectral artifacts that result in low SC values. The lowering of the SC values occurs because the signal present at the hot pixels is not real although it may appear to be a real feature at first glance. The most easily discernible difference between the benchtop and handheld spectra occurs at ~1417 cm^{-1} where the library spectrum does not contain a feature but the control and commercial sets do. Figure 4 shows the Raman spectral comparison of famciclovir without hot pixels. Elimination was performed using an in-house algorithm that involves the application of a median filter with a 15-point window to the spectral regions surrounding the hot pixels. The algorithm was applied to the handheld spectra to eliminate the hot pixels in the data acquired on the handheld Raman for the control and commercial sets. The corrected Raman spectra without hot pixels were used for SC comparison between with the library set spectrum. The SC values shown in Table III were above 0.90 for all samples except two: ciprofloxacin commercial (manufacturer 2, set 1) and a metronidazole control, which were 0.889 and 0.895, respectively. As in the NIR study, the results show that spectral library signatures chosen to populate the library are representative of the supply chain for each particular drug. A typical Raman pass–fail screen is shown in Figure 5.

Conclusions

This study shows that library-based SC methods can be used to screen finished products in a nondestructive and rapid fashion. The NIR and Raman results indicate that both types of portable techniques can be used to perform reliable screening of finished products. The broader implications of this study indicate that libraries can be built on different NIR and Raman spectrometers and transferred successfully to field units. These techniques are straightforward and allow for use by nonexperts. Spectral libraries can be used with portable NIR and Raman spectrometers in a field setting, thereby providing an efficient way to increase the number of products that undergo physical testing before reaching consumers in the event of a global pandemic.

Acknowledgments

This project was supported in part by the Center for Drug Evaluation and Research (CDER) Critical Path and Regulatory Science & Review Enhancement Programs. The project was supported in part by an appointment (C.V.N) to the Research Participation Program at the CDER administered by the Oak Ridge Institute for Science and Education (ORISE) through an interagency agreement between the U.S. Department of Energy (DOE) and U.S. Food and Drug Administration (FDA).

Disclaimer

This article reflects the views of the authors and should not be construed to represent the FDA's views or policies.

References

(1) A. Patel and S.E. Gorman, *Clin. Pharmacol. Ther.* **86**, 241–243 (2009).
(2) P.H. Merrell, L. Buhse, and J.D. Rodriguez, *Tablets and Capsules* **11**, 22–26 (2013).
(3) J.D. Rodriguez, C.M. Gryniewicz-Ruzicka, J.F. Kauffman, S. Arzhantsev, A.L. Saettele, K.A. Berry, B.J. Westenberger, and L.F. Buhse, *Am. Pharm. Review* **16**, 9–18 (2013).
(4) Y.L. Loethen and J.D. Rodriguez. *Am. J. Anal. Chem.* **6**, 559–568 (2015).
(5) F.H. Long, *Handbook of Stability Testing in Pharmaceutical Development* (Spectroscopic Solutions, LLC, New Jersey, 2009), chap. 11, pp. 223–239.
(6) M. Kayat, G. Ritchie, S. Pieters, C. Heil, R. Kershner, R. Cox, G.L. Reid, and M. Mabry, *Am. Pharm. Rev.* September/October (2012).
(7) J.D. Rodriguez, B.J. Westenberger, L.F. Buhse, and J.F. Kauffman, *Analyst* **136**, 4232–4240 (2011).
(8) K.M. Morisseau and C.T. Rhodes, *Pharmaceutical Research* **14**(1), 108–111 (1997).
(9) C.M. Hodges and J. Akhavan, *Spectrochim. Acta, Part A* **46**(2), 303–307 (1990).
(10) G. Reich, *Adv. Drug Delivery Rev.* **57**(8), 1109–1143 (2005).
(11) S.H.F. Scafi and C. Pasquini, *Analyst* **126**, 2218–2224 (2001).
(12) J.S. Day, H.G.M. Edwards, S.A. Dobrowski, and A.M. Voice, *Spectrochim. Acta, Part A* **60**(3), 563–568 (2004).
(13) M.D. Hargreaves, K. Page, T. Munshi, R. Tomsett, G. Lynch, and H.G.M. Edwards, *J. Raman Spectrosc.* **39**(7), 873–880 (2008).
(14) R. McCreery, *Chem. Anal.* **157,** 193 (2000).

Dr. Chelliah V. Navin is a Research Fellow in the U.S. FDA Division of Pharmaceutical Analysis in St. Louis, Missouri. **Dr. Latevi Lawson** develops and improves on both the analytical and statistical methodologies for the rapid screening team with the FDA's Department of Pharmaceutical Analysis. **Dr. Jason D. Rodriguez** is a Research Chemist in the FDA Division of Pharmaceutical Analysis. Direct correspondence to: Jason.Rodriguez@fda.hhs.gov

This article originally appeared in *Spectroscopy,* **31**(s9), 8–15 (2016).

DISCRIMINATION OF BACTERIAL GROWTH MEDIA USING PORTABLE RAMAN SPECTROSCOPY WITH BACKGROUND FLUORESCENCE SUBTRACTION

Jessica A. Randall and Mathew G. Lyman

We investigated the feasibility of identifying different types of bacterial growth medium using a handheld Raman instrument with a proprietary baseline correction algorithm. Our data suggest that this instrument is capable of differentiating multiple types of growth medium and readily detects the change in the Raman signal when bacteria are present in the growth medium. These findings support the notion that a handheld Raman spectrometer may be used to distinguish highly-fluorescent biological samples without the use of surface-enhanced Raman scattering.

In the field of forensic sciences, handheld Raman spectrometers are used by the military and first responders for the rapid identification of unknown substances (1–3). These unknown materials include toxic industrial chemicals (TICs), toxic industrial materials (TIMs), chemical warfare agents, explosives, narcotics, pharmaceutical compounds, and plastics. However, Raman spectroscopy has historically been problematic for the identification of biological samples, such as bacteria, growth media, and tissues. Sample fluorescence typically overwhelms Raman scattering by several orders of magnitude, resulting in a high background and poor spectral matching (4).

Two general methodologies have been used to detect weak Raman signals from biological organisms and materials: surface-enhanced Raman scattering (SERS) and fluorescence background subtraction (also known as *baseline correction*). SERS is a technique that boosts the signal of Raman-active molecules when measured on customized metal surfaces, typically gold, silver, and copper (5,6). The increase in Raman signal on these metals is often dramatic, usually on the order of 10^4–10^6, but it can be as high as 10^{11} (7,8). Therefore, increasing the Raman signal over background fluorescence allows the Raman spectra to be discretely visible. In fact, a number of publications have shown that different types of bacteria and growth media have unique SERS spectra, thereby establishing SERS as a potential pathogen diagnostic tool despite the intrinsic fluorescence of the sample (9–22).

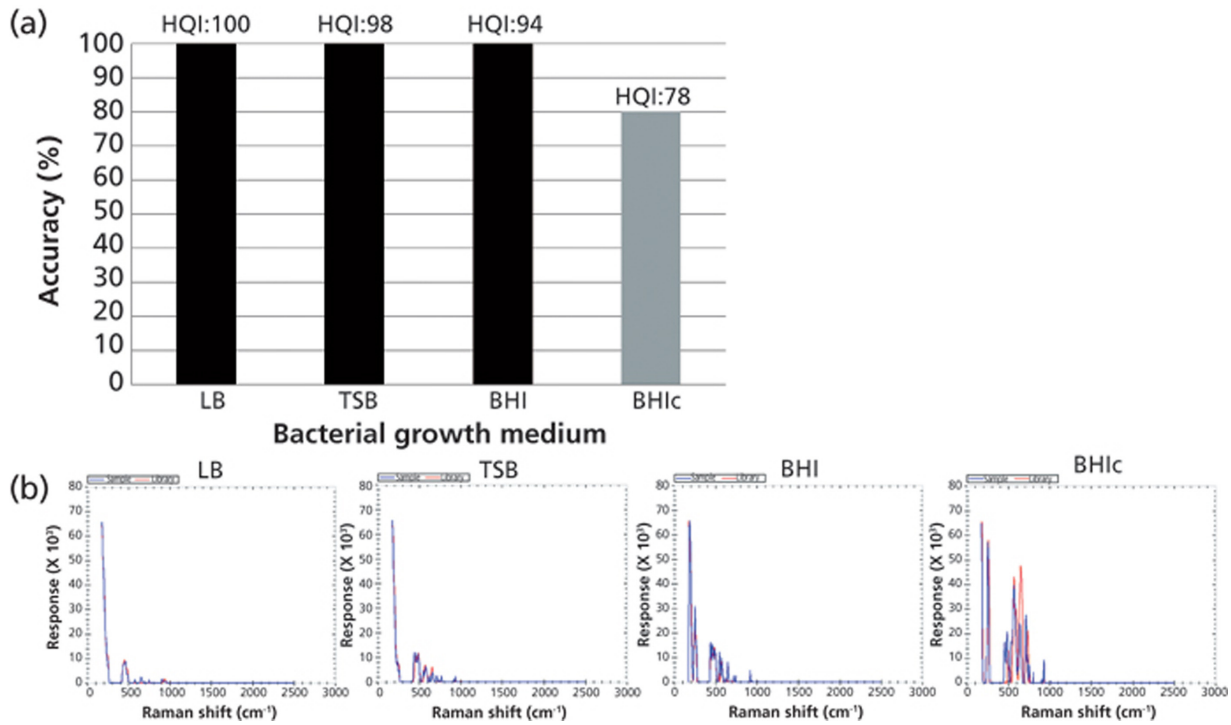

Figure 1: (a) Measuring the accuracy of the portable spectrometer on four types of bacterial growth medium: LB, TSB, BHI, and BHIc. Scans were recorded as a "match" if the instrument correctly identified the medium as the top match with an HQI value ≥ 90. Scans that exceeded this average value are shown in black, while scans below this threshold value are show in grey. (b) Representative overlays of the baseline-corrected sample spectrum (blue line) and the library spectrum (red line) are shown for each of the four types of growth medium.

Fluorescence background subtraction is a second option for "teasing out" a weak Raman signal from fluorescent biological samples. In contrast to SERS, fluorescence background subtraction does not increase Raman signal during acquisition; it differentiates it computationally by deducting the background fluorescence from the Raman signal post-acquisition. Several computational methods have been developed for background subtraction from Raman spectra, including background estimation using computational geometry (23), principal component analysis (24), wavelet transformation (25–30), polynomial fitting (4,31–36), frequency-domain filtering (37), and first-order and second-order differentiation (38,39).

In this study, we investigated the feasibility of fluorescence background subtraction using a handheld spectrometer to differentiate several bacterial growth media, specifically in the presence and absence of bacteria. As SERS is often not practical for first responders and military personnel (because of time constraints, limited dexterity in personal protective equipment, and ease of use), we tested

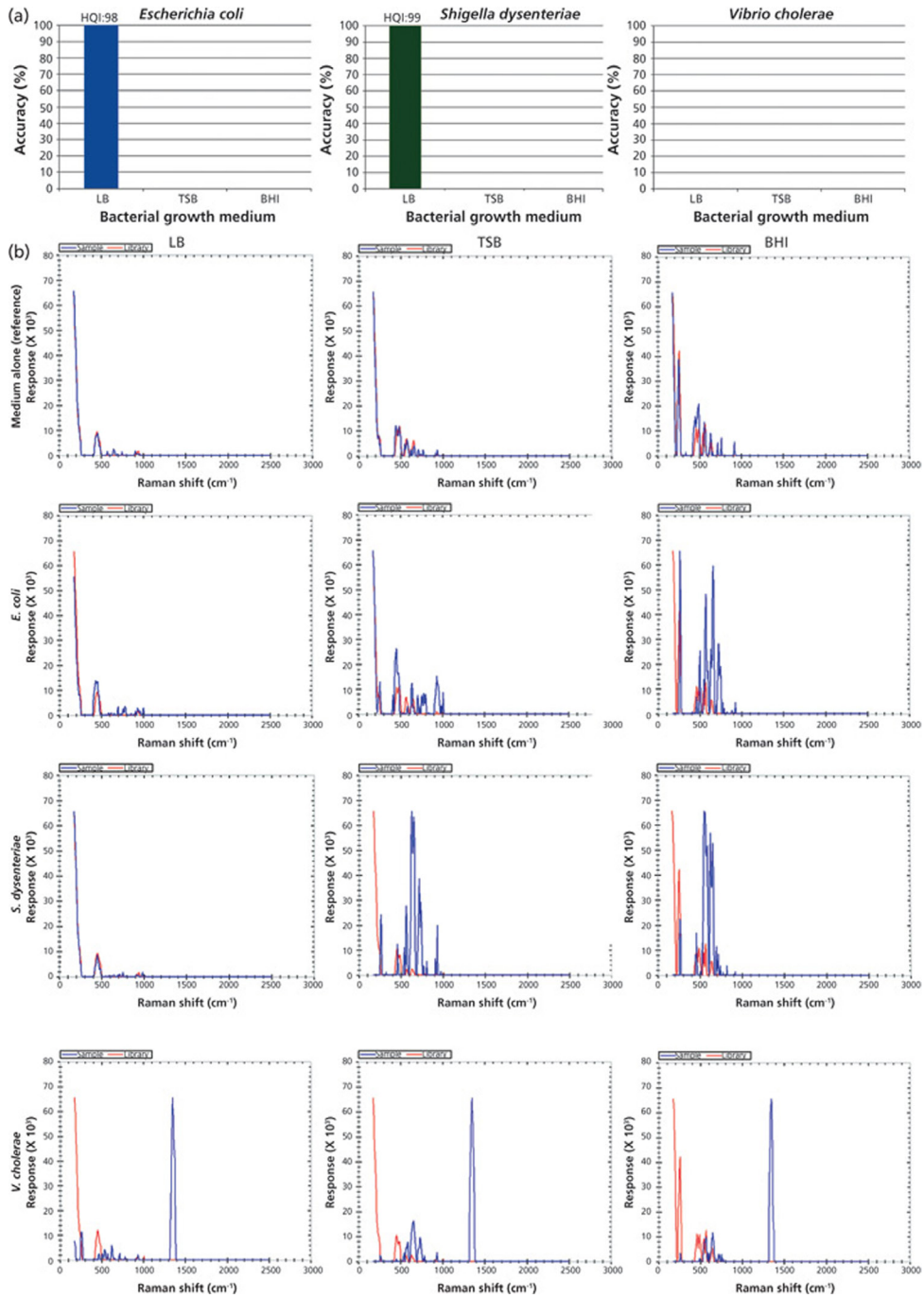

Figure 2: (a) Culturing *Escherichia coli, Shigella dysenteriae,* and *Vibrio cholerae* in LB, TSB, or BHI markedly decreased the accuracy rate of the portable spectrometer to match to the growth medium spectra in the library. (b) Representative overlays of the baseline-corrected sample spectrum (blue line) and the library spectrum (red line) are shown for each of the three types of growth medium in the presence of *Escherichia coli, Shigella dysenteriae,* and *Vibrio cholerae*. The medium alone scan (reference) is unadulterated growth medium matched to itself.

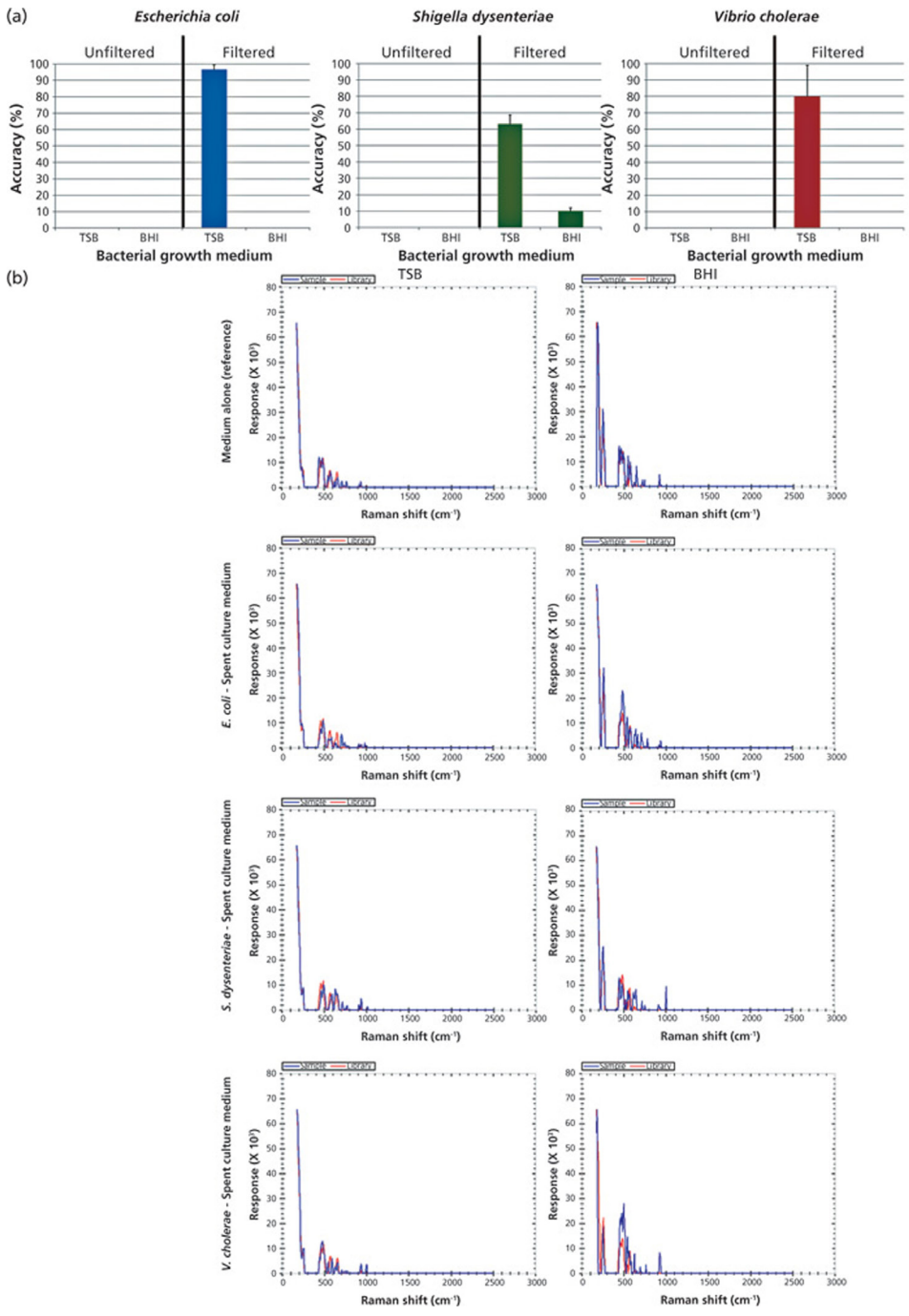

Figure 3: (a) Removing bacteria from culture medium partially restores the ability of the handheld spectrometer to match to the growth medium spectra in the library. (b) Representative overlays of the baseline-corrected spent culture medium (blue line) and the library spectrum (red line) are shown for TSB and BHI after *Escherichia coli, Shigella dysenteriae,* and *Vibrio cholerae* have been filtered from the culture.

a portable Raman spectrometer that utilizes a proprietary algorithm to subtract background fluorescence. This baseline correction capability may allow for the interrogation of biologic materials that would otherwise "swamp" traditional handheld Raman instruments used in forensic analyses.

Experimental Conditions

Handheld Raman Spectrometers

A NanoRam handheld spectrometer was obtained from B&W Tek, Inc. The operation presets were as follows: excitation wavelength = 785 nm, laser power = 90% (270 mW), number of hits displayed = 3, and spectral range = 176–2900 cm^{-1}. For sample analysis, the spectrometer was fitted with the vial adaptor for 4-mL glass vials.

Bacterial Growth Media

Four types of bacterial growth media were analyzed for this study: LB-Miller broth, tryptic soy broth (TSB), brain heart infusion (BHI) broth, and brain heart infusion-cysteine (BHIc) broth. All base media were purchased from Becton Dickinson and prepared according to the manufacturer's recommendations. BHIc medium required additional supplementation as reported previously (40). Briefly, 1 L of BHI medium (37 g/L) containing cysteine (1 g/L) was sterilized following the manufacturer's recommendations. The following supplements were then prepared and added before use: β-nicotinamide adenine dinucleotide (β-NAD) (1 mg/mL — dissolve 200 mg β-NAD in 200 mL of deionized water, filter sterilize using a 0.2-µm filter, store at 4 °C), heme-histidine (1 mg/mL — add 200 mg of L-histidine, 200 mg of hemin-HCl and 4 mL of 1 N NaOH to 196 mL of deionized water; microwave briefly to dissolve; filter sterilize; store at 4 °C away from light), and glucose (25 mL, 20% w/v). All BHIc supplements were purchased from Sigma-Aldrich.

Table I: Individual components of bacterial growth media analyzed in this study

LB-Miller Broth (per L)	Tryptic Soy Broth (per L)	Brain Heart Infusion Broth (per L)	BHIc Broth (per L)
Trytone (10 g)	Pancreatic digest of Casein (17 g)	Calf brains, infusion from 200 g (7.7g)	Calf brains, infusion from 200 g (7.7g
Yeast extract (5 g)	Papaic digest of soybean (3g)	Beef heart, infusion from 250 g (9.8 g)	Beef heart, infusion from 250 g (9.8 g)
Sodium chloride (10 g)	Dextrose (2.5 g)	Proteose peptone (10 g)	Proteose peptone (10 g)
	Sodium chloride (5 g)	Dextrose (2 g)	Dextrose (2 g)
	Dipotassium phosphate (2.5 g)	Sodium chloride (5 g)	Sodium chloride (5 g)
		Disodium phosphate (2.5 g)	Disodium phosphate (2.5 g)
			Cysteine (1 g)
			β-Nicotinamide adenine dinucleotide (10 mL, 1 mg/mL)
			Heme-histidine (10 mL, 1 mg/mL)
			Glucose (25 mL, 20% w/v)

Raman Spectroscopy of Bacterial Growth Media

For Raman spectroscopy of bacterial media, 1 mL of LB-Miller broth, TSB, BHI, and BHIc media were transferred to separate 4-mL screw-cap glass vials (Fisher). Each medium sample was then added to a "User Defined Library." For the handheld spectrometer, a unique Raman spectrum for each medium was captured and added to the library. After the user library was established, each medium vial was subsequently analyzed an additional 10 times (n = 10) to determine if

the spectrometer could distinguish between the different growth media. The accuracy rate and hit quality index (HQI) value (that is, confidence score) for the 10 iterations were then recorded.

Raman Spectroscopy of Bacterial Cultures

Overnight cultures were set up in each medium with three different organisms: *Escherichia coli* C3000 (obtained from Oklahoma State University), *Shigella dysenteriae* (BEI number NR-520), and *Vibrio cholerae* (BEI number NR-144). A loopful of frozen glycerol stock was used to inoculate 5 mL of each medium in a 50-mL vented flask (Cellstar) and cultured for 18 h at 37 °C with shaking. Then, 1 mL of each sample was analyzed (n = 10) and matched against the User Defined Library. Scans were recorded as a "match" if the instrument correctly identified the medium as the top match and an HQI ≥ 90. If there were no hits, or the instrument did not correctly identify the compound, it was recorded as a "no-match." The accuracy rate and HQI value (that is, confidence score) for the 10 iterations were then recorded. The bacterial titer for each culture was calculated by performing serial 10-fold dilution and spotted onto tryptic soy agar (TSA) culture plates (20 µL/spot) in triplicate for each sample and dilution. Plates were incubated under aerobic conditions at 37 °C and the colony forming units (cfu) were calculated. The titers for Escherichia coli in LB, TSB, and BHI were 5×10^8, 9.5×10^8, and 4.5×10^8 cfu/mL, respectively. The titers for Shigella dysenteriae in LB, TSB, and BHI were 3×10^6, 1×10^8, and 8×10^7 cfu/mL, respectively. The titers for Vibrio cholerae in LB, TSB, and BHI were 9.0×10^7, 1.3×10^8, and 2.5×10^8 cfu/mL, respectively.

Raman Spectroscopy of Filtered Bacterial Cultures (Spent Culture Medium)

Overnight cultures were started in LB, BHI, and TSB media with *Escherichia coli* C3000, *Shigella dysenteriae,* and *Vibrio cholerae* as described previously. The following day, bacteria were removed from the cultures using a 50-mL Millipore sterile disposable vacuum filtration unit with a 0.22-µm PES membrane. The resulting filtered media samples were then analyzed (n = 10) by the handheld Raman instrument in replicate experiments (three separate cultures).

Data Analysis

All data scans were downloaded from the handheld Raman instrument into NanoRam ID Client v3.10 software. In ID Client, each overlay (sample scan and library match) was reviewed and a representative scan was chosen for each data set. Screen shots of the data scans were then captured and imported into Photoshop CS5 software (Adobe) where they were cropped and organized into figures. All graphing was performed in Microsoft Excel software.

A notable limitation of the handheld instrument is displaying a library spectrum with a sample spectrum that has a low HQI value (does not match). By default, the instrument displays the sample spectrum overlaid with the library spectrum that has the highest HQI value (the best match). Therefore, to have the instrument overlay

a library spectrum with a dissimilar sample spectrum (for the purpose of demonstration in the figure), we created some user libraries with only a single medium entry (for example, unadulterated BHI was entered into a user library and used to match bacterial cultures propagated in BHI; even though the Raman spectra were dramatically different, the instrument would overlay the library spectrum of BHI alone with the sample spectrum of BHI and the bacteria).

Results

To investigate the utility of using a handheld Raman spectrometer for identifying bacterial medium (Figure 1), we tested four different types of growth medium with increasing complexity: LB-Miller Broth (LB), Tryptic Soy Broth (TSB), Brain-Heart Infusion Broth (BHI), and a complex derivative of BHI used for culturing *Francisella tularensis* (BHIc). The ingredients for each medium are listed in Table I.

The accuracy rate (%) was determined by interrogating 10 sample replicates for each type of medium. Scans were recorded as a "match" if the instrument correctly identified the medium as the top match in the library, and the HQI value was ≥ 90. The HQI value indicates how well the unknown scan matches to the library scan; an HQI of 100 indicates an identical match while lower values indicate the dissimilarity between scans (41). As shown in Figure 1a, the NanoRam spectrometer was able to match LB, TSB, and BHI media with 100% accuracy with HQI values ≥ 94. BHIc, the most complex medium in the study, matched with 80% accuracy with an average HQI value of 78. Figure 1b shows a representative spectrum from each medium analyzed. Scans for LB, TSB, and BHI were nearly identical to the library scans (blue tightly fit to red). However, the spectrum for the BHIc medium was more variable compared to the library spectrum (red visible with no blue), indicating that the match was of lower quality. These findings suggest that the NanoRam is likely able to match to a variety of bacterial growth media using its proprietary background subtraction algorithm. However, analyzing highly-complex medium such as BHIc results in lower HQI values.

After determining that the instrument was able to distinguish between different types of growth medium, we investigated whether culturing three types of enteric bacteria (*Escherichia coli, Shigella dysenteriae,* and *Vibrio cholerae*) dramatically affected the Raman spectra compared to culture medium alone. We also assessed whether these three types of bacteria could be visually distinguished from one another by their subtracted Raman spectra (as a proof-of-principle). *Escherichia coli, Shigella dysenteriae,* and *Vibrio cholerae* were cultured in LB, TSB, and BHI; these cultures were then analyzed by the NanoRam spectrometer to compare spectra of broth alone and broth containing bacteria. Interestingly, both the *Escherichia coli* and *Shigella dysenteriae* cultures in LB matched, with 100% accuracy, to the library scans of

LB medium alone (Figure 2a). A similar finding was observed by Premasiri and colleagues (18), who noted that "media containing extracts from other micro-organisms such as yeast extract" showed a similar appearance to SERS spectra of bacterial cells, an observation consistent with culturing these bacteria in LB (a yeast extract base). By contrast, spectra from cultures of *Escherichia coli, Shigella dysenteriae,* and *Vibrio cholerae* in TSB and BHI were notably different than those of medium alone, and did not match the library spectra (Figure 2a). Figure 2b shows the Raman spectra of LB, TSB, and BHI alone (reference scans, first row) compared to the three enteric bacteria cultured in these media (rows 2–4). Note that the red library scan, for each of the representative Raman plots, was from pure medium alone (LB, TSB, or BHI); the blue sample scan represents the change in the Raman spectrum from the bacterial culture relative to medium alone. Although *Escherichia coli* and *Shigella dysenteriae* cultured in LB had similar scans relative to LB alone, all three bacteria showed unique background-subtracted Raman spectra in TSB and BHI, suggesting that it may be feasible to distinguish between multiple types of bacteria cultured in a variety of growth media using a handheld Raman spectrometer without using SERS.

Next, we investigated whether the robust Raman peaks observed in the bacterial cultures from Figure 2 were caused exclusively by the presence of the bacteria, or whether the Raman-active components in the growth medium had also changed during bacterial growth. We hypothesized that if the dramatic changes in Raman spectra were due to bacteria alone, filtering out these bacteria from the spent culture medium would restore the ability of the handheld Raman spectrometer to match to the "medium alone" library scans, specifically for TSB and BHI (bacterial cultures that had a 0% match rate for all three bacteria). To test this hypothesis, overnight bacterial cultures were grown to saturation. Cultures were then filtered through a 0.22-µm membrane to remove bacteria; spent culture media were then analyzed using the handheld Raman spectrometer (Figure 3a). Filtering out the bacteria largely restored the ability of the instrument to match TSB spent culture medium to the original TSB library scan (with an HQI value ≥ 90), whereas the BHI spent culture medium did not match to the library scan at the original HQI threshold. However, most of the BHI scans had HQI values ranging from 75 to 89, suggesting that the BHI spent culture medium was similar to unadulterated BHI. Representative scans also supported the notion that the spent culture medium had minor differences in their Raman spectra compared to the original growth medium, although these differences were enough to drop the HQI value below our threshold for a match (Figure 3b). These data suggest that the bacteria in the culture medium are primarily responsible

for the dramatic change in the background-subtracted Raman spectra compared to medium alone.

Discussion and Conclusion

We investigated whether a handheld Raman instrument that subtracts background fluorescence was able to identify increasingly complex bacterial growth medium, with and without bacteria. We found that the instrument was effective in identifying several types of traditional growth medium at an HQI value of ≥ 90, but was less accurate with complex specialty mediums, such as BHIc. In addition, culturing bacteria in these media resulted in markedly different Raman spectra compared to media alone, suggesting that it may be feasible to distinguish between multiple types of bacteria cultured in a variety of growth media if an on-board reference library is generated first. We also noted variability in the intensity and position of peaks in replicate spectra for each condition, suggesting that if a reference library were to be generated, each library spectrum would need to be an average of multiple scans (ideally).

Two recent studies have discussed the use of SERS to differentiate bacterial growth medium and different species of bacteria (that is, by boosting the Raman signal during acquisition) (16,18). We show in this study that growth medium and bacteria could also be differentiated using a fluorescence background subtraction algorithm post-acquisition. This is particularly relevant for first responders and military personnel who use handheld Raman spectrometers to identify chemicals (TICs), toxic industrial materials (TIMs), chemical warfare agents, explosives, and narcotics, but historically struggle with "bio" materials because of their high background fluorescence. Therefore, future studies will build upon these initial findings and investigate the ability of handheld Raman spectrometers to correctly identify a multitude of crude bacterial cultures, purified bacterial cells (washed), as well as dried spores.

References

(1) H. Markert, J. Rings, N. Campbell, and K. Grates, N. F. S. T. Center, Ed. (National Institute of Justice, Largo, Florida, 2011), pp. 1–8.

(2) W. Smith, P. White, C. Rodger, and G. Dent, in *Handbook of Raman Spectroscopy: From the Research Laboratory to the Process Line,* I.R. Lewis and H. Edwards, Eds. (Marcel Dekker, New York, New York, 2001).

(3) V. Otieno-Alego and N. Speers, in *Infrared and Raman Spectroscopy in Forensic Science,* J.M. Chalmers, H. Edwards, and M. Hargreaves, Eds. (John Wiley & Sons Ltd, West Sussex, UK, 2012).

(4) C.A. Lieber and A. Mahadevan-Jansen, *Appl. Spectrosc.* **57**, 1363 (2003).

(5) M. Culha, B. Cullum, N. Lavrik, and C. Klutse, *J. Nanotechnol.* **2012**, 15 (2012).

(6) B. Sharma, R. Frontiera, A. Henry, E. Ringe, and R. Van Duyne, *Mater. Today* **15**, 16 (2012).

(7) K. Kneipp, H. Kneipp, I. Itzkan, R. R. Dasari, and M.S. Feld, *Chem. Rev.* **99**, 2957 (1999).

(8) K. Kneipp, H. Kneipp, I. Itzkan, R.R. Dasari, and M.S. Feld, *Curr. Sci.* **77**, (1999).

(9) H. Chu, Y. Huang, and Y. Zhao, *Appl. Spectrosc.* **62**, 922 (2008).

(10) J.A. Guicheteau, K. Gonser, and S.D. Christesen, A.P.G. National Research Council Associate at the U.S. Army ECBC Research Lab, Ed. (U.S. Government, Edgewood, 2004).

(11) R.M. Jarvis, A. Brooker, and R. Goodacre, *Anal. Chem.* **76**, 5198 (2004).

(12) R.M. Jarvis and R. Goodacre, *Anal. Chem.* **76**, 40 (2004).

(13) M. Kahraman, M.M. Yazici, F. Sahin, and M. Culha, *J. Biomed. Opt.* **12**, 054015 (2007).

(14) M. Kahraman, M.M. Yazici, F. Sahin, and M. Culha, *Langmuir* **24**, 894 (2008).

(15) T.T. Liu et al., *PLoS One* **4**, e5470 (2009).

(16) N.E. Marotta and L.A. Bottomley, *Appl. Spectrosc.* **64**, 601 (2010).

(17) I.S. Patel, W.R. Premasiri, D.T. Moir, and L.D. Ziegler, *J. Raman Spectrosc.* **39**, 1660 (2008).

(18) W.R. Premasiri, Y. Gebregziabher, and L.D. Ziegler, *Appl. Spectrosc.* **65**, 493 (2011).

(19) W.R. Premasiri et al., *J. Phys. Chem. B* **109**, 312 (2005).

(20) W.R. Premasiri, D.T. Moir, M.S. Klempner, and L.D. Ziegler, Eds., *New Approaches in Biomedical Spectroscopy,* (Oxford University Press, New York, 2007).
(21) A. Sengupta, M.L. Laucks, and E.J. Davis, *Appl. Spectrosc.* **59**, 1016 (2005).
(22) L. Zeiri, B.V. Bronk, Y. Shabtai, J. Eichler, and S. Efrima, *Appl. Spectrosc.* **58**, 33 (2004).
(23) N. Kourkoumelis, A. Polymeros, and M. Tzaphlidou, *Spectrosc. Int. J.* **27**, 311 (2012).
(24) T. Hasegawa, J. Nishijo, and J. Umemura, *Chem. Phys. Lett.* **317**, 642 (2000).
(25) T.T. Cai, D. Zhang, and D. Ben-Amotz, *Appl. Spectrosc.* **55**, 1124 (2001).
(26) C. Camerlingo, F. Zenone, G.M. Gaeta, R. Riccio, and M. Lepore, *Meas. Sci. Technol.* **17**, 298 (2006).
(27) Y. Hu et al., *Chemom. Intell. Lab. Syst.* **85**, 94 (2007).
(28) J. Li, L.P. Choo-Smith, Z. Tang, and M.G. Sowa, *J. Raman Spectrosc.* **42**, 580 (2011).
(29) P.M. Ramos and I. Ruisánchez, *J. Raman Spectrosc.* **36**, 848 (2005).
(30) Z. Zhang et al., *J. Raman Spectrosc.* **41**, 659 (2010).
(31) B.D. Beier and A.J. Berger, *Analyst* **134**, 1198 (2009).
(32) A. Jirasek, G. Schulze, M.M. Yu, M.W. Blades, and R.F. Turner, *Appl. Spectrosc.* **58**, 1488 (2004).
(33) M.N. Leger, A.G. Ryder, *Appl. Spectrosc.* **60**, 182 (2006).
(34) V. Mazet, C. Carteret, D. Brie, J. Idier, and B. Humbert, *Chemom. Intell. Lab. Syst.* **76**, 121 (2005).
(35) T.J. Vickers, R.E. Wambles, and C.K. Mann, *Appl. Spectrosc.* **55**, 389 (2001).
(36) J. Zhao, H. Lui, D.I. McLean, and H. Zeng, *Appl. Spectrosc.* **61**, 1225 (2007).
(37) P.A. Mosier-Boss, S.H. Lieberman, and R. Newbery, *Appl. Spectrosc.* **49**, 630 (1995).
(38) A. O'Grady, A.C. Dennis, D. Denvir, J.J. McGarvey, and S.E. Bell, *Anal. Chem.* **73**, 2058 (2001).
(39) D. Zhang and D. Ben-Amotz, *Appl. Spectrosc.* **54**, 1379 (2000).
(40) P. Mc Gann et al., *J. Microbiol Methods* **80**, 164 (2010).
(41) J. Kauffman, J.D. Rodriguez, and L.F. Buhse, *Am. Pharm. Rev.* **14**, (2011).

Jessica A. Randall and **Mathew G. Lyman** are with the Chemical, Biological, Radiological, Nuclear, and Explosives Division at Oklahoma State University – University Multispectral Laboratory in Ponca City, Oklahoma. Direct correspondence to: mlyman@okstate-uml.org

This article originally appeared in *Spectroscopy,* **28**(s6), 8–19 (2013).

Fast and Selective Detection of Trigonelline, a Coffee Quality Marker, Using a Portable Raman Spectrometer

Angeline Saldaña Ramos, Yulán Hernandez, and Betty C. Galarreta
Chemistry Department, Catholic University of Peru (Pontificia Universidad Católica del Perú)

Quality control in the food industry is a key issue that requires rapid, efficient, and selective methods that could discriminate the products, detect fraudulent or accidental adulterations, and identify the content of some biomarkers within a particular process of storage conditions. Along these lines, Raman spectroscopy in conjunction with the optical properties of metallic nanostructures is a powerful technique that can be implemented in food analysis.

Surface-Enhanced Raman Spectroscopy (SERS) is a technique that takes advantage of the optical properties of noble metal nanostructures (e.g., gold or silver nanospheres) to enhance the Raman signals of molecules adsorbed on the surface of the metal. Changes in the material, geometry, and size of the metallic structures enable the modulation in enhancement of these unique nanoantennas. This advance has led to many applications, including the design of new and selective sensors with lower limits of detection for food metabolites in order to adapt to agriculture and industry needs. In addition, SERS minimizes acquisition time and reduces the amount of sample needed.

In this regard, this report shows how the portable Raman device i-Raman Plus 785 can be used in combination with modified gold nanotriangles to develop an alternative quantification method for trigonelline. This alkaloid is a biomarker present in different food items, such as coffee and quinoa, that provides potential health benefits and whose thermal degradation (e.g., during the roasting of green coffee beans) makes the formation of different flavor and aroma compounds possible. For example, a coffee brew could contain around 2.3 mM of trigonelline, and there could be around 30–65 µmol of trigonelline in one gram of green coffee beans, which would be an indicator of quality and could be tested using this technique.

Gold nanotriangles modified with mercaptopropionic acid have been used as nanoantennas to quantify the concentration of trigonelline solutions from the SERS signal. The nanostructures have been optimized to enhance signals between 700 and 800 nm wavelength.

Calibration curves have been prepared using the 1034-cm-1 peak area and compared with traditional Raman spectroscopy. The results show the advantages of the technique, which include lower limits of detection, and the potential of this method for quantifying trigonelline in food.

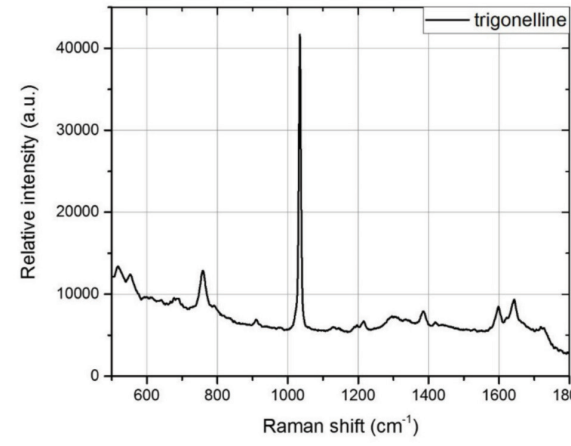

Figure 1: Raman spectrum of trigonelline solution at 250 mM.

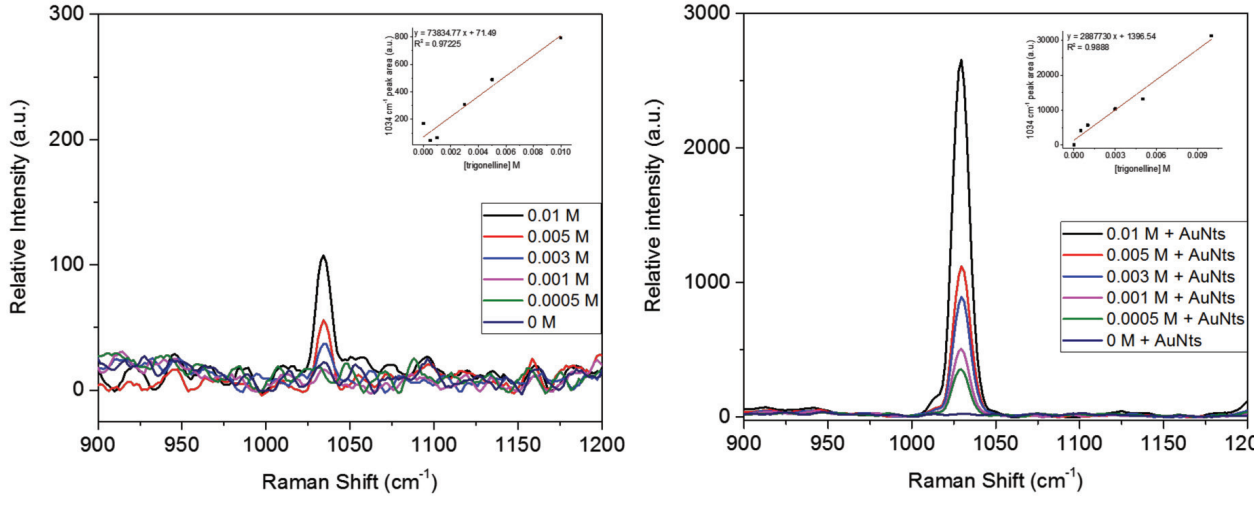

Figure 2: Raman spectra of trigonelline solutions without gold nanotriangles (left) and with gold nanotriangles (right). Inserts show the calibration curves of trigonelline solutions using the 1034 cm^{-1} peak area within a 1010–1045-cm^{-1} spectral window.

Experimental

Instrumentation: i-Raman Plus portable spectrometer with 785-nm laser excitation (BWS465-785H), Raman shift range of 150–2800 cm-1, 50-sec integration time, 10 scans, and a liquid cuvette holder (BCR100-A) with 10-mm optical path.

Samples: Standard trigonelline aqueous solutions ranging from 10.0 mM to 0.5 mM. Gold nanotriangles modified with mercaptopropionic acid and suspended in deionized water (AuNTs).

Results and Discussion

A 250-mM solution of trigonelline was analyzed using conventional Raman spectroscopy. The spectrum in Figure 1 shows an intense signal at 1034 cm-1, corresponding to the pyridine ring breathing mode, which could be used to monitor the concentration of this compound in water.

Four independent sets at five different concentrations were analyzed within the 0.5-mM and 10-mM range by conventional Raman spectroscopy and by SERS. The latter one requires an extra step where the modified gold nanotriangles are mixed with the trigonelline solutions (trigonelline: gold nanotriangles = 15:2) before samples are scanned. In all cases, the strong signal observed at 1034 cm^{-1} was monitored and the peak area within the 1010–1045-cm^{-1} spectral window was used to determine the concentration of the alkaloid. Based on the results and the calibration curves (see Figure 2), it was possible to observe an improvement on the signal to noise ratio of SERS over the conventional Raman spectra under the same experimental conditions. The results show it is possible to detect concentrations below 0.5 mM using this method.

In summary, we describe a simple method to quantify the presence of diluted trigonelline in solutions using surface enhanced Raman spectroscopy as a tool that could potentially improve the quality control process of food items such as coffee and quinoa.

References

- B.C. Galarreta, Y. Hernandez, and A. Saldaña Ramos, "Síntesis y aplicación de nanotriángulos de oro en el desarrollo de un método de cuantificación de un potencial alcaloide terapéutico: la trigonelina" ["Synthesis and application of gold nanotriangles in the development of a quantification method of a potential therapeutic alkaloid: trigonelline"] Dirección de Gestión de la Investigación (DGI-2016-352) PUCP.
- B.C. Galarreta and H. Maruenda, "Espectroscopía vibracional y de resonancia magnética nuclear en el control de calidad de café orgánico peruano y café instantáneo" ["Vibrational spectroscopy and nuclear magnetic resonance in the quality control of Peruvian organic coffee and instant coffee"] Dirección de Gestión de la Investigación (DGI-2014-078) PUCP.
- R. Aroca, *Surface-Enhanced Vibrational Spectroscopy* (J. Wiley & Sons, Hoboken, New Jersey, 2016).
- A. Jaworska et al., *Vibrational Spectroscopy* 63, 469–476 (2012).

Further Reading

Portable Raman for SERS Applications
Choosing the Most Suitable Laser Wavelength
Analysis of Edible Oils by a Portable Raman Spectrometer

Additional Resources

Raman Spectroscopy Overview
i-Raman Plus Datasheet
Portable Raman for Agricultural Products &
Cultural Heritage in Peru